

A comparative study of jet substructure taggers

Paloma Quiroga-Arias

LPTHE, UPMC Univ. Paris 6 and CNRS UMR7589, Paris, France

Sebastian Sapeta

IPPP, Durham University, South Rd, Durham DH1 3LE, UK

Abstract

We explicitly study how jet substructure taggers act on a set of signal and background events. We focus on two-pronged hadronic decay of a boosted Z boson. The background to this process comes from QCD jets with masses of the order of m_Z . We find a way to compare various taggers within a single framework by applying them to the most relevant splitting in a jet. We develop a tool, **TOY-TAG**, which allows one to get insight into what happens when a particular tagger is applied to a set of signal or background events. It also provides estimates for significance and purity. We use our tool to analyze differences between various taggers and potential ways to improve the performance by combining several of them.

1 Introduction

The substructure of boosted hadronically-decaying objects differs from that of pure QCD jets whose mass falls in a compatible invariant mass window. Therefore the usefulness of boosted jet substructure techniques for the identification of hadronically decaying massive objects such as W/Z bosons [1], Higgs boson [2–8] or the top quark [2, 9–11] (for review see [12]). The existing procedures, such as filtering [3], pruning [11] or trimming [13], extract the internal structure of jets by using information from the clustering procedure. Those substructure algorithms are able to distinguish between heavy resonances and pure QCD contributions, therefore allow for enhancing signal to background ratio.

In the last years, there has been a proliferation of new taggers which are used for the identification and cleaning of signal versus background (for the most recent review see [14]). We have also already seen an impressive variety of experimental studies using these techniques [15–17]. Though obviously (subtle in some cases) differences exist between various taggers and combining them may lead to an enhanced statistical power [7, 18], there must be a significant amount of overlap between them as they are often based on very similar principles. Unfortunately, full algorithmic implementations of the taggers are complex and if one further combines several taggers and optimizes them the whole procedure becomes a black box with very limited possibility to gain an understanding of what actually happens to the ensemble of the signal and background events.

In this paper we perform a study of a selection of the most commonly used tagging methods in an attempt to understand and characterize where the differences in the various definitions come from and to what substructure features the different outcome after applying the taggers can be attributed. In order to make it possible, and to some extent analytically trackable, we perform some approximations to the tagger definitions and apply them to Monte Carlo simulations of a signal and the corresponding background processes.

From such simulations we take the hardest (fat) jet, which in the case of signal corresponds to the hadronic decay of the boosted heavy resonance, and we analyze its substructure and the performance of the various taggers. For that purpose, we developed an interactive tagging tool, **TOY-TAG**, which allows one to apply different taggers to the desired signal and background files *in a user friendly way*.

The paper is organized as follows. In the next section we describe how we simulate our signal and background events, which approximations we make to the mass of jets (sec. 2.2) and we introduce

the concept or relevant splitting (sec. 2.3) that will enable us to analyze all the taggers in the same framework. The tagger definitions and the approximations we apply to them are given in sec. 2.4. In sec. 3 we introduce our **TOY-TAG** tool and make some comparisons to the exact implementations of the taggers. The tool is then used in sec. 4 to discuss differences between taggers and to study how they perform in term of purity and significance, also in the case with combinations of taggers. We summarize our work in sec. 5.

2 Study of taggers on Monte Carlo simulations

Our aim is to explicitly study how the taggers act on a set of statistically significant ensemble of signal and background events. We will focus on two-pronged hadronic decays of boosted electroweak bosons reconstructed using fat jet substructure techniques.¹ The background to this process will be coming from QCD jets whose mass is comparable with that of a signal jet.

2.1 Event simulation and reconstruction

We have generated several million proton-proton collisions at nominal LHC energy $\sqrt{s}=14$ TeV for the processes $Z+\text{jet}$ ($\rightarrow l^+l^-+\text{jet}$) and ZZ ($\rightarrow l^+l^-+\text{hadrons}$) using Pythia 6.4 [19]. The event generation was done at hadron level with the underlying event switched off. The latter can be justified by the fact that, as shall be explained in the following subsection, our implementations of the taggers will analyze directly the most relevant splitting in a jet. The original implementations, however, iterate over many splittings until they get to the one which is the most relevant. On the way to that splitting, they remove significant part of the underlying event. Since we access the most relevant splitting directly, we do not have the mechanism of UE removal. Therefore, our implementations of the taggers acting on the events without UE approximately correspond to the original taggers acting on the events with UE. We performed jet reconstruction using either the k_t [20] or the Cambridge/Aachen (C/A) [21, 22] sequential recombination algorithm with $R=1$ (so that both products of the decay of the heavy object belong to the same jet), as implemented in FastJet 3.0.1 [23–25]. Different values of the cut for the jet transverse momentum $p_{T,\text{min}}$ were used between 400 and 800 GeV and the window for the mass of the hardest jet was imposed at $70 < m_J < 110$ GeV. For both processes we look for the lepton pair from the decay of the boson that reconstructs its mass, and in the opposite hemisphere there is a fat jet which is kept if its mass falls within the stated window. In the case of ZZ , such fat jet corresponds to our signal, that is the hadronic decay of the boson, while in $Z+\text{jet}$ constitutes the background, with a QCD jet faking the mass of a Z boson, and therefore the substructure of such jet is different from the genuine decay.

2.2 Mass of a jet and the relevant splitting

Amongst all the splittings that one finds in a signal jet, there is one which is special since it does not come from a QCD branching but from a decay of a heavy object. This splitting is responsible for most of the mass of a jet and the substructure techniques are designed to search for it in order to separate signal from background. Therefore, we will refer to it as the *relevant splitting* throughout the paper. During the jet clustering procedure, the relevant splitting corresponds to the merging of two subjets, which we will call J_1 and J_2 , into the jet J . The two main characteristics of this merging (splitting) are

$$z = \frac{p_{T,J_1}}{p_{T,J}}, \quad \Delta = \sqrt{(y_{J_1} - y_{J_2})^2 + (\phi_{J_1} - \phi_{J_2})^2}, \quad (1)$$

and the mass of the jet J can be expressed in terms of these variables to be approximately

$$m_J^2 \simeq z(1-z)p_{T,J}^2\Delta^2 + m_{J_1}^2 + m_{J_2}^2. \quad (2)$$

Let us now briefly consider what approximations are made to get to the above formula. The exact mass of a jet, expressed in terms of its two parent subjets, is given by

$$m_{J,\text{exact}}^2 = 2m_{T,J_1}m_{T,J_2} \cosh(y_{J_2} - y_{J_1}) - 2p_{T,J_1}p_{T,J_2} \cos(\phi_{J_2} - \phi_{J_1}) + m_{J_1}^2 + m_{J_2}^2. \quad (3)$$

¹A hadronically decaying boosted heavy object is seen as a single (large radius, therefore ‘fat’) jet. Such jet is called a W-jet or Z-jet when the heavy object is an EW boson.

	$\delta_1(\%)$	$\delta_2(\%)$	$\delta_3(\%)$	$\delta_4(\%)$	$\sigma_{\delta,1}$	$\sigma_{\delta,2}$	$\sigma_{\delta,3}$	$\sigma_{\delta,4}$
Z-jet								
$p_T=200$ GeV	5.0	4.9	7.3	12.9	2.9	3.4	3.6	5.7
$p_T=400$ GeV	5.2	5.1	5.9	11.9	3.2	3.3	3.5	6.0
QCD-jet								
$p_T=200$ GeV	7.8	7.8	10.0	17.8	3.7	4.1	4.2	6.2
$p_T=400$ GeV	8.9	8.8	9.7	18.4	4.3	4.5	4.7	6.6

Table 1: Amount by which the mass of a jet is underestimated when taking the different approximations from Eqs. (4)–(7).

When $m_{J1(J2)} \ll p_{T,J1(J2)}$, the mass of the jet can be approximated by

$$m_{J,\text{app1}}^2 = 2p_{T,J1}p_{T,J2} \left[\cosh(y_{J2} - y_{J1}) - \cos(\phi_{J2} - \phi_{J1}) \right] + m_{J1}^2 + m_{J2}^2. \quad (4)$$

This holds well if the two subjets have commensurate transverse momenta. However, for asymmetric jets there is a significant correction to this approximation. If we further assume that the radius of our jet R is small we get

$$m_{J,\text{app2}}^2 = p_{T,J1}p_{T,J2}\Delta^2 + m_{J1}^2 + m_{J2}^2, \quad (5)$$

with Δ defined by Eq. (1). This works well for sufficiently boosted jets. For Z-jets a transverse momentum of 400 GeV gives validity to this approximation (see table 1 for the numbers as a function of p_T). The next step is to use the variable $z = p_{T,J1}/p_{T,J}$ and assuming $p_{T,J2} = (1-z)p_{T,J}$

$$m_{J,\text{app3}}^2 = z(1-z)p_{T,J}^2\Delta^2 + m_{J1}^2 + m_{J2}^2. \quad (6)$$

This is rather innocent as compared to the other approximations that we have just discussed, especially in a boosted regime, where it does not introduce more than a 3% error. One can make further approximation by dropping the masses of the subjets

$$m_{J,\text{app4}}^2 = z(1-z)p_{T,J}^2\Delta^2. \quad (7)$$

This is equivalent to having a two massless particle jet, and it is a reasonable assumption in the case of a signal jet, because, as it has been already stated, its mass comes mainly from the relevant splitting.

To estimate the error introduced by each level of approximation, we calculate the percentage by which the mass is misestimated, averaging over all the events considered, and the corresponding standard deviation

$$\delta_i = \frac{m_J - m_{J,\text{app}i}}{m_J}, \quad \sigma_{\delta,i}. \quad (8)$$

The results are summarized in table 1. Both the Z-jet and QCD events were produced at $\sqrt{s} = 14$ TeV and selected with the [70, 110] GeV mass window. No tagging was applied at this stage. We see that the approximations corresponding to Eqs. (6) or (7) lead to $\mathcal{O}(10\%)$ average effect on the mass of the signal jets and $\mathcal{O}(20\%)$ for the background QCD jets (for the jets which pass the above mass window selection cut).

Since we aim at performing the study of taggers in an analytic way, approximations are necessary. After analysing the effects of different degrees of approximation on the mass distributions, in what follows we will use the results from Eqs. (6) or (7).

2.3 Optimal determination of the relevant splitting

In our analysis we will be interested in identifying the relevant splitting out of the fat jet substructure in simulated events. Each event will be labelled with the (z, Δ) pair corresponding to such splitting in order to study how signal and background events differ from each other and how much of that difference is captured by various tagging techniques.

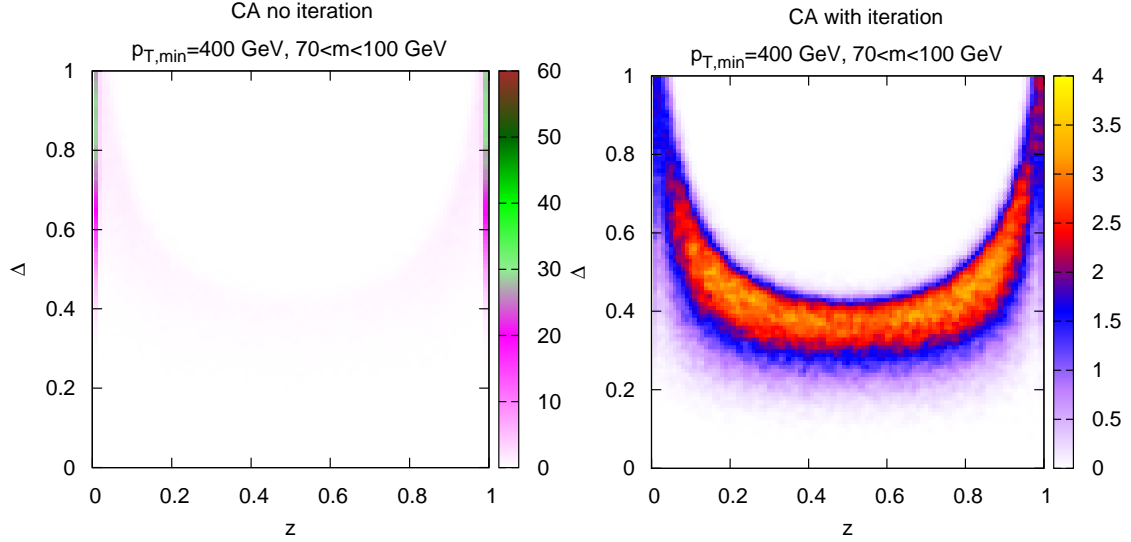


Figure 1: Unclustering of the hardest jet with C/A algorithm. Left: just one step in the unclustering process. Right: iteration in the unclustering process until the relevant splitting is found (see text for more detailed explanation). The vertical axis, whose values are represented by the color gradient to the right of each plot, represent the cross section $\frac{d\sigma}{dzd\Delta}$ in femtobarns.

Depending on which jet finding algorithm we take, the subjets coming from the relevant splitting are merged at a different stage of its clustering. Therefore, it is important to choose an algorithm which allows one to get to this splitting as easily as possible and without biasing the sample. Since we are interested only in the infrared and collinear safe algorithms with well defined jet substructure, the choice is limited to either C/A [21, 22] or k_t [20] jet algorithms.

The mass of a jet, Eq. (2), involves both the distance between its two subjets, Δ , and the ratio of the subjet transverse momentum to the p_T of the jet, $z = p_{T,\text{subjet}}/p_{T,\text{jet}}$. The subjet used to compute this ratio is chosen randomly from the two available subjets. Hence, sometimes it is the softer and sometimes the harder one. Therefore z is in the range $[0, 1]$. For a fat jet resulting from the hadronic decay of a heavy object, both z and Δ are relatively large for the relevant splitting. Since the measure of the k_t algorithm involves both of these variables and is the largest when the two are maximal, one expects that the relevant splitting will correspond to the last merging for the k_t algorithm. This is not necessarily the case for the Cambridge/Aachen algorithm since its measure involves nothing but the geometric distance Δ .

To show that this is indeed the case, we performed the following study. We generated a sample of boosted jets from the hadronic decay of a Z boson with the selection criteria described in sec. 2.1² and the cut on transverse momentum of the hardest jet $p_{T,\text{min}} = 400$ GeV. Next we proceeded to analyse the substructure of those jets, applying the same procedure to the k_t and C/A algorithms. We unclustered the last step of the algorithm and used the two resulting subjets to determine z and Δ . Then we dropped the lighter of the two subjets and repeated the above steps for the heavier subjet. We continued this procedure each time checking before unclustering whether our jet's mass was above 70 GeV. In the case in which the mass dropped below 70 GeV we stopped iterating and stored the corresponding (z, Δ) pair as a final value in the histogram. The purpose of this analysis was to identify the relevant splitting, the main idea being that if our unclustering happens at the relevant splitting the mass of the heavier subjet should drop significantly below 70 GeV.

In Fig. 1 we show the corresponding results for the C/A algorithm. The left histogram was obtained after just one unclustering so it corresponds to the last merging in the clustering sequence regardless of whether or not this merging is the relevant one. On the contrary, on the right hand side, the values of z and Δ correspond to the relevant splitting determined with the iteration

²The MC generation of events is done with the underlying event turned off. We have repeated the same exercise for ZZ with the underlying event as well for Zj with Z decaying leptonically, each time finding the same behaviour as for the case of ZZ with no UE described below.

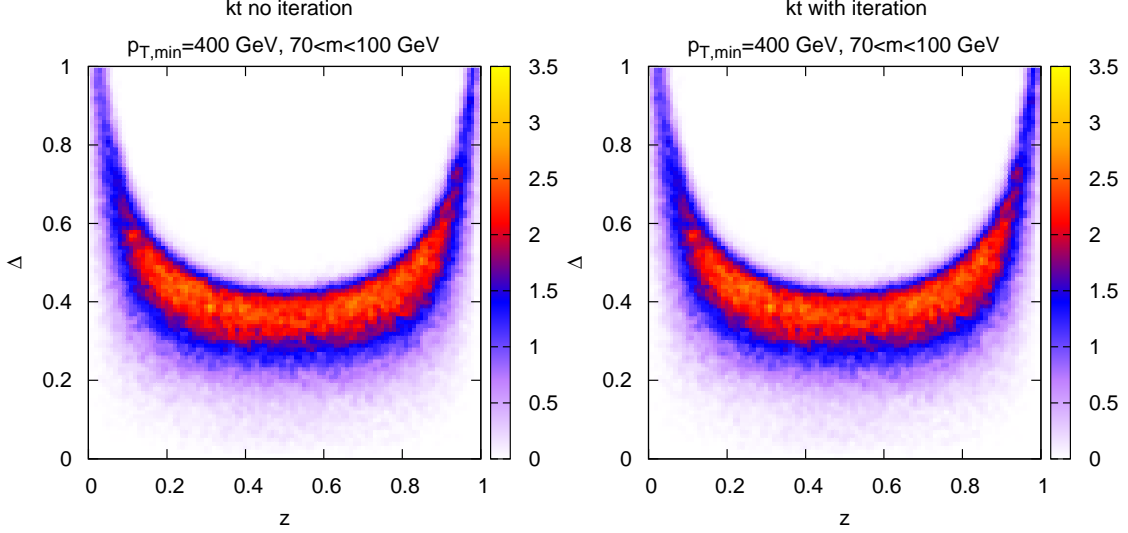


Figure 2: Same as in Fig. 1 but for the k_t algorithm.

procedure described above. The two plots differ drastically which tells us that the last merging in the C/A algorithm is hardly ever the relevant one. Most of the time it is just a large angle merging of highly asymmetric objects.

This picture looks very different for the k_t algorithm as shown in Fig. 2. Here, the histograms obtained after just one unclustering and, alternatively, after the relevant splitting was identified, are basically the same. This suggests that for the k_t algorithm the last splitting is most of the time the relevant one. In other words, the (z, Δ) pair of the two subjects from the first unclustering in the k_t algorithm should account for most of the mass of a jet.

We remark that it was this feature of the k_t algorithm that was exploited by the seminal papers on jet substructure [1,2]. It also makes the k_t algorithm particularly suitable for our further study of the taggers since it allows one to get the z and Δ of the relevant splitting directly and obtain a tagger-independent profile of an ensemble of events which then can be used to study how various taggers act on the signal and background events.

2.4 Taggers under study: definitions and approximations

As mentioned before, each event of the Monte Carlo simulation is labelled with the (z, Δ) pair of variables³ corresponding to its relevant splitting and it is added to a 2D colour map such as those shown in section 2.3 (see Fig. 1 and 2). For this purpose, and following the discussion from the previous section, we have used the k_t -algorithm unclustering so that no iteration is needed. As we have already mentioned, the original formulations of the majority of the taggers use the C/A algorithm, and therefore iterations are needed. By making such choice the jets get cleaned in the process of finding the relevant splitting throughout the iterations along the splitting process: in each iteration the lightest of the two subjects is dropped, which is equivalent to removing soft radiation. This cleaning process does not take place when using k_t -unclustering. As we shall see in section 3.1, where both C/A with iterations and k_t without iterations are used in MC simulations, these two methods lead to similar results. In order to study the performance of different tagging techniques, we consider analytic definitions of the taggers and take the necessary approximations, if any, so that they can be represented within the same setup as the MC simulations, that is with each tagger shown as a line which corresponds to a certain constant value of the tagging parameter.

The taggers considered in this study and the approximations made to facilitate the analytic consideration and the consequent representation in the (z, Δ) plane together with the Monte Carlo simulations, are presented next. For each of the taggers we include the criteria applied in order to keep signal and reject background events. Whenever the condition is satisfied, the event is kept.

1. Mass drop

³It's Δ/R , but we have always used $R=1$.

As its name suggests, this tagger imposes a cut to the ratio of the mass of the heavier of the subjects (J1) to the mass of the jet [3, 4]

$$\frac{m_{J1}^2}{m_J^2} < \mu_{\text{cut}}^2, \quad (9)$$

to be accepted as a signal jet. Therefore, in order to apply such tagger, it is necessary to consider (at least) the heavier of the subjects as massive, so one needs to go beyond the first approximation and take the mass of the jet to be

$$m_J^2 = z(1-z)p_{TJ}^2\Delta^2 + m_{J1}^2, \quad (10)$$

otherwise the tagger would be always trivially passed. m_{J1} in the above equation is the mass of the heavier subjet. In what follows, we shall choose it to be constant and we shall fix it at some average value that will be extracted from Monte Carlo. Once normalized to the mass of the jet m_J , we have the following formula for the mass drop parameter as a function of the variables (z, Δ)

$$1 - \Delta^2 z(1-z) \frac{p_{TJ}^2}{m_J^2} < \mu_{\text{cut}}^2. \quad (11)$$

One thing that follows from the above formula and Eq. (10) is that there is a minimal value of μ_{cut}^2 below which the mass drop tagger (within our approximation) will have no effect on an event ensemble. This minimal value corresponds to the point $\Delta = 1$ and $z = \frac{1}{2}$ and is given by $\mu_{\text{cut}, \text{min}}^2 = 1/(1 + p_{TJ}^2/(4m_{J1}^2))$. This will act as a limitation of our current approximation of this tagger and it will be less and less relevant for high values of p_{TJ} .

2. Asymmetry cut

This tagger eliminates the most asymmetric configurations which generate big masses but are most commonly coming from QCD radiation and not from the decay of a heavy object. It is defined as [3]

$$\frac{p_{TJ}^2}{m_J^2} \min(z^2, (1-z)^2) \Delta^2 > y_{\text{cut}}. \quad (12)$$

In what follows, as in the case of mass drop, we shall use that formula (10) for the mass of the jet. That sets the upper limit for the values of the tagger parameter which is $y_{\text{cut}, \text{max}} = 1/(1 + 4m_{J1}^2/p_{TJ}^2)$. As we shall see later, this limit will have no practical importance for the range of the jet transverse momenta of interest. We note that, unlike in the case of the mass drop, the asymmetry cut is nontrivial even in the massless subjet approximation to the jet mass from Eq. (7). However, as we shall see in sections 3 and 4, by using finite m_{J1} , we reproduce important features of the original implementation of this tagger.

3. Jade distance normalized to p_{TJ}

The approximation to the jet mass from Eq. (7) suggests the use of the Jade distance [26, 27] to construct the tagger which rejects all jets whose two subjects are too close according to the Jade measure. In order to get a dimensionless condition, we can normalize the Jade distance to the transverse momentum of the jet. This leads to a criterion which neither depends on the jet mass nor its p_T , but only on the ratio of the transverse momentum of the subjet to the p_T of the jet, z , and the separation between subjects⁴, Δ ,

$$z(1-z)\Delta^2 > J_{p_T, \text{cut}}. \quad (13)$$

The viable range for the values of this tagger is $J_{p_T, \text{cut}} \in [0, \frac{1}{4}]$. We note that if we chose to normalize our Jade distance to the mass of the jet we would have effectively reproduced the mass drop condition from Eq. (11).

4. Modified Jade distance normalized to p_{TJ}

Similarly, a modified version of the Jade distance can be used to construct a tagger, as was proposed in [4]. If we normalize it to the transverse momentum of a jet we get

$$z(1-z)\Delta^4 > J_{\text{mod}, \text{cut}}. \quad (14)$$

Similarly to the previous version of the Jade tagger, also here, the limits for the values of the parameter are $J_{\text{mod}, \text{cut}} \in [0, \frac{1}{4}]$.

⁴It really is Δ/R but, once again, this study is restricted to $R=1$.

5. 1-subjettiness

N-subjettiness [28, 29] exploits the fact that the pattern of the hadronic decay of a heavy object is reflected through the presence of distinctive energy lobes corresponding to the decay products, as opposed to QCD jets which present a more uniformly spread energy configuration (not aligned along the subjet axis). The inclusive jet shape N-subjettiness is defined, in its generalized version as derived in [30], as

$$\tau_N = \frac{1}{d_0} \sum_k p_{T,k} \min((\Delta R_{1,k})^\beta, \dots, (\Delta R_{N,k})^\beta),$$

where k runs over the constituent particles in the jet, $\Delta R_{J,k} = \sqrt{(\Delta y)^2 + (\Delta\phi)^2}$, β corresponds to an angular weighting exponent, and the normalization factor is $d_0 = \sum_k p_{T,k} R^\beta$ with R being the jet radius. The discriminating variable used when applying N-subjettiness in the identification of two-prong hadronic objects is the ratio τ_2/τ_1 , which turns out to be smaller for signal than for background. However, since in our simplified configuration we are considering the subjets with no substructure, we can only consider the 1-subjettiness measurement, τ_1 , without introducing additional variables that would not allow us to represent this tagger in a (z, Δ) map. In other words, we have a jet ($N = 1$) with two constituent particles ($k = 2$) whose distances to the jet axis satisfy $\Delta R_{1,1} + \Delta R_{1,2} = \Delta$.

Therefore, we restrict ourselves to the 1-subjettiness case, which has the following functional form in terms of the characteristic variables z and Δ

$$\Delta^\beta (z(1-z)^\beta + z^\beta(1-z)) > \tau_{1,\text{cut}}. \quad (15)$$

The consideration of just τ_1 for 2-prong hadronic objects, though not optimal, is still meaningful, since the value of τ_1 for a Z-jet will be larger than that of a QCD-jet. The viable range for the values of this tagger is $\tau_{1,\text{cut}} \in [0, \frac{1}{2}]$.

6. Pruning

Pruning [10, 11] was designed to identify signal over background configurations and at the same time to clean the former. By definition it modifies the jet substructure in order to reduce the systematic effects that obscure the reconstruction of hadronic heavy objects. It takes the constituents of a jet putting them through a new clustering procedure in which each of the branchings is requested to pass a set of cuts on kinematic variables. If the cuts are not passed, then the recombination is vetoed and one of the two branches is discarded. The conditions for each recombination $i, j \rightarrow p$ are

$$\frac{\min(p_{T,i}, p_{T,j})}{p_{T,p}} < z_{\text{cut}} \quad \text{AND} \quad \Delta R_{ij} > D_{\text{cut}}.$$

If both conditions are met, the merging does not take place and the softer branch is discarded. One then continues the procedure with the remaining branch. For the purpose of this study, similarly to what we have done for the other taggers, we apply the pruning based criteria to the relevant splitting only. That is, we require

$$\min(z, 1-z) > z_{\text{cut}} \quad \text{OR} \quad \Delta < D_{\text{cut}}, \quad (16)$$

for an event to be accepted. The dynamic condition on Δ is defined as

$$D_{\text{cut}} = 2D \frac{m_J}{p_{TJ}}, \quad (17)$$

which results, if one takes the mass of the jet as given by Eq. (10), in the following condition for pruning

$$\min(z, 1-z) > z_{\text{cut}} \quad \text{OR} \quad \Delta < \frac{m_{J1}}{p_{TJ} \sqrt{\frac{1}{4D^2} - z(1-z)}}, \quad (18)$$

for the event to pass, with m_{J1} being the mass of the most massive of the two subjets. The parameters of the tagger can vary in the ranges $z_{\text{cut}} \in [0, \frac{1}{2}]$ and $D \in (0, p_{TJ}/(2m_J)]$. Note however, that for $D > 1$ the expression inside the square root in Eq. (18) will become zero and then negative for some range around $z = \frac{1}{2}$. This essentially means that the condition for

Δ is always satisfied in this region of z . One needs to keep in mind that while this modified pruning still presents the signal to background discriminatory power, it is oblivious to its original capabilities to clean the signal jets that allowed for a more accurate reconstruction and an improved mass resolution.

7. Trimming

This tagging procedure reclusters jet constituents into subjets with radius R_{sub} and then discards the contributions from subjets which do not satisfy the condition

$$p_{T,i} > f_{\text{cut}} \Lambda_{\text{hard}}, \quad (19)$$

where f_{cut} is a fixed dimensionless parameter and Λ_{hard} is some characteristic hard scale.

In the case of our simplified configurations of two subjets at relevant splitting, the trimming condition takes the form

$$\min(z, 1-z) > \frac{f_{\text{cut}} \Lambda_{\text{hard}}}{p_{TJ}}, \quad (20)$$

and assuming that for most of the jets $p_{TJ} \simeq p_{T,\text{min}}$, the above condition is nothing but a special case of pruning from Eq. (18) with $D_{\text{cut}} = D_{\text{cut,min}}$.

The taggers from the above list were defined by various authors in contexts of different studies. Admittedly however, the effect they have on a given ensemble of events is not independent for each of them. It is difficult to quantify the amount of overlap between different taggers in general. However, it is possible to find a common ground on which the taggers can be compared if some approximations are applied to them. We believe that the approximations presented in this section grasp the most essential features for each tagger.

Already at this point we can make several interesting observations. First of all, the asymmetry cut, as can be seen from Eqs. (10) and (12), involves not only the ratio of transverse momenta of the subjets to the p_T of the jet, z or $1-z$, but also the distance between them Δ . It is therefore also rejecting those jets whose subjets at the relevant splitting are geometrically too close to one another. In other words it is doing part of the job of the group of taggers based on mass of the jet like mass drop or Jade distances. This is important since the asymmetry cut and the mass drop are often used together.

It is also interesting to note in this context that the asymmetry cut kicks in before the mass drop. This is because the former affects already the simplest possible jet consisting of two massless partons in which case the condition from Eq. (12) takes the form $\min(\frac{z}{1-z}, \frac{1-z}{z}) > y_{\text{cut}}$. On the other hand, the same simplest configuration can never be rejected by the mass drop tagger since the condition from Eq. (9) is always trivially satisfied for the case with $m_{J1} = 0$. Hence, for the mass drop to start having an effect, at least one of the subjets has to have its own substructure which produces its non-zero mass.

By comparing Eqs. (18) and (19) we can see that we should expect some amount of overlap between pruning and trimming, at least in some subregions of the parameter spaces of those taggers.

3 Interactive tagger tool TOY-TAG

We have developed an interactive tool, **TOY-TAG**, that allows the user to apply the different taggers defined in section 2.4, separately or in combinations, to the desired signal and background files which come in the form of a 2D surface plots for the (z, Δ) values of the relevant splitting (sec. 2.3). The script, available from <http://www.ippp.dur.ac.uk/~sapeta/toytag>, allows one to vary the values of the tagging parameters upon user request as well as the minimum transverse momentum of the jet. We have implemented all the taggers from section 2.4 except for trimming. This is because, as discussed in sec. 2.4, to the accuracy we are working in, the former is just a special case of pruning.

Since the information contained in the data files used by **TOY-TAG** is limited to the values of z and Δ for the relevant splitting, for those taggers presenting an explicit dependence of the transverse momentum and mass of the jet some minimal modelling is necessary. Since the cross section drops drastically with increasing transverse momentum we set $p_{TJ} = p_{T,\text{min}}$. Concerning the mass, in order to bring the performance of the **TOY-TAG** as close as possible to real tagging, in our implementation, the mass of the more massive of the two subjets is taken into account as indicated by Eq. (10)

$$m_J^2 \simeq z(1-z)p_{TJ}^2\Delta^2 + m_{J1}^2,$$

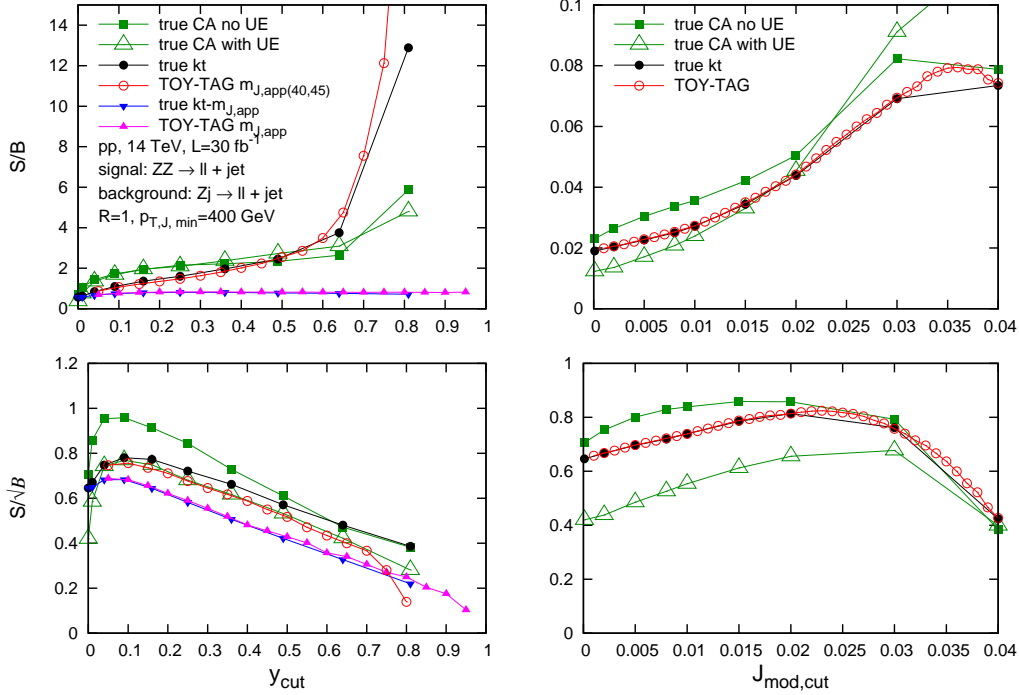


Figure 3: Comparison of TOY-TAG to exact taggers. S/B (upper row) and S/\sqrt{B} (lower row) for y_{cut} , Eq. (12) (left panel), and $J_{\text{mod, cut}}$, Eq. (14) (right panel). The minimum transverse momentum in the event sample used to produce this plot is $p_{T,\text{min}}=400$ GeV. The label “TOY-TAG $m_{J,\text{app}}$ ” refers to results obtained using the TOY-TAG with the approximation of Eq. (7) for the mass of the jet while the label “TOY-TAG $m_{J,\text{app}(40,45)}$ ” corresponds to the TOY-TAG using the mass approximation given by Eq. (10) with $m_{J1}=40$ and 45 GeV for signal and background respectively. Results labelled as “TOY-TAG” correspond to the case in which there is no dependence on m_J and $p_{T,J}$ and therefore no extra modelling is needed. The meaning of the rest of the labels is explained in the text.

with m_{J1} being the mass of the heavier of the two parent subjets, which will be set to a constant. In order to determine the value of m_{J1} , we have studied the mass distribution of the heavier of the subjets in Monte Carlo simulations (results not shown). The average mass of a subjet turns out to be larger for the background than for the signal. The numerical values used in TOY-TAG are given in the following subsection.

The TOY-TAG allows one not only to directly study which subgroups of events are rejected by a particular tagger or a combination of taggers both for signal and background jets, but also to get a first estimate of purity, S/B , and significance, S/\sqrt{B} . Those quantities are computed by integrating the 2D histograms in (z, Δ) above (or in the case of pruning below) the line $\Delta = f(z)$, which is a representation of each tagger in this plane. A concrete illustration will be given in sec. 4.

3.1 Comparison to exact implementations of the taggers

After all the simplifications that were necessary in order to construct a simple tool which makes it possible to perform comparisons between various tagger, it is interesting to check how realistic is the description provided by TOY-TAG. We do this by computing the values of signal to background and signal to square root of background for different taggers using TOY-TAG and comparing them to the results from Monte Carlo simulations in which the taggers were rigorously applied. The latter means using the exact definitions of the taggers, unclustering with the C/A algorithm and using iteration along the splitting chain until the tagging criteria is satisfied.

As argued in section 2.1, TOY-TAG should be applied to events without UE since it does not have the cleaning stage. In order to illustrate how big the effects of UE are and to give some estimate of a potential uncertainty associated with it, we applied the exact taggers both to events with and without UE, labeled as “true CA with UE” and “true CA no UE” respectively.

Also, in order to directly cross check our implementation and to quantify the role played by the approximations adopted by **TOY-TAG**, we run the MC simulation in which the taggers were applied to the first splitting using the k_t -algorithm with no further iteration (see discussion in section 2.3). Such results are labelled “true kt”. On top of this, for those taggers including explicitly a dependence on the jet mass, **TOY-TAG** needs further approximation, as explained at the beginning of sec. 3. In order to account for this extra approximation, we run the MC simulation using the approximate value of m_J which is used by **TOY-TAG**, Eq. (10), and these results are referred to as “true kt- $m_{J,\text{app}}$ ”.

In Fig. 3, we show the results for signal to background and signal to square root of background for two different taggers:⁵ one independent of the mass and transverse momentum of the jet, modified Jade distance normalized to p_T , Eq. (13), and another one, the asymmetry cut, that has a dependence on m_J and p_{TJ} and hence requires further modelling. The results shown in the figure correspond to the luminosity $L = 30 \text{ fb}^{-1}$. For **TOY-TAG** we consider different levels of approximations explained before.

We have found the values of the correction for the mass of the heaviest subjet, Eq. (10), by optimizing the behaviour of S/B and S/\sqrt{B} as compared with tagging in MC. As mentioned earlier, we also studied exact masses of subjets from Monte Carlo simulations. We can assert that the values for m_{J1} found by optimizing Eq. (10) implemented in the **TOY-TAG** are consistent with the actual masses of the subjets, being larger for a QCD-jet than for a Z-jet. They are equal to 45 GeV and 40 GeV, for the background and the signal subjets respectively. Also, the fact that this values are weakly dependent on the transverse momentum of the jet is in agreement with the results of the MC study. We repeat that even though taking the constant value of m_{J1} is a somewhat crude approximation, it allows us to reproduce important features of the exact versions of the taggers and at the same time enables us to gain some understanding by being able to analytically study and compare the taggers in their simplified forms. By introducing the parameter m_{J1} , which has the meaning of the average mass of the hardest subjet, we mimic the real situation with massive subjets and therefore the discussion based on our implementations of the taggers becomes more realistic.

For taggers independent of m_J and p_{TJ} , like the modified Jade distance normalized to p_{TJ} , shown in Fig. 3 (right), the performance of the **TOY-TAG** is very accurate up to large values of the tagging parameter, in which the iteration process in the original C/A formulation starts making a difference. **TOY-TAG** describes perfectly the results obtained in MC when applying the tagger with k_t -unclustering.

In the case of taggers with explicit dependence on mass and p_{TJ} , the situation is more complicated and a more careful interpretation of the results is in place. As shown in Fig. 3 (left), we find perfect agreement for the y_{cut} tagger between the **TOY-TAG** and MC when in both cases the mass of the jet is approximated by Eq. (7), rejecting any mass contribution from the constituent subjets (“ $m_{J,\text{app}}$ ” label in the plot). However, the results thus obtained are far from those obtained from “true kt” and “true CA” on MC, especially in the case of S/B . When the mass of the subjet is taken into account in **TOY-TAG**, Eq. (10), its performance improves significantly, successfully describing the MC results from tagging with k_t -unclustering (“true kt”). There are still some differences between improved **TOY-TAG** (and “true kt”) compared to the original tagger formulations with the C/A algorithm, “true CA”. Especially S/B for the asymmetry cut tagger starts to be very sensitive to the absence of iterations (in “true kt” and **TOY-TAG**) for large value of y_{cut} . This is understandable since by requiring high y_{cut} we have less chances of finding a sufficiently symmetric splitting in the background jet and that is why S/B grows. The reason why the growth of S/B with y_{cut} is smaller in the case of C/A (hence for the case with iterations) is that by going deeper into the substructure of a jet we increase the chance of finding a splitting which satisfies the condition of the tagger. That will matter much more for the background jet since its probability for the relevant splitting to be symmetric is much smaller than in the case of a signal jet. We can therefore conclude at this point that if the y_{cut} tagger is implemented with the k_t -algorithm (and therefore iterations play a minor role), the **TOY-TAG** gives a very accurate results for S/B and S/\sqrt{B} . If however the C/A version of the asymmetry tagger is used, then the result from **TOY-TAG** will be misestimated near the lower and the upper limit of y_{cut} , still reproducing however the correct qualitative behaviour.

⁵These validation study has been performed for all the taggers included in **TOY-TAG**. Though only two taggers are shown, the results found are consistent for all of them, and the discussion in this section is applicable to all of them.

We performed similar validation study for all the taggers implemented in **TOY-TAG**. We have concluded that the agreement between the performance of **TOY-TAG** and the true tagging applied to Monte Carlo simulations stays within 40% except for the values of the parameters near the limits where only the qualitative behaviour of the taggers can be trusted.

In particular, the agreement for the significance, S/\sqrt{B} , is quite good for all taggers and all values of the tagging parameter, with the exception of the mass drop tagger which for values of $\mu < 0.5$, i.e. a very strict tagging, shows larger deviations. This is expected since the mass drop is the only tagger which requires, by definition, second order corrections (the fact that the mass of the constituent subjets must be considered) and is directly related to the value of $\mu_{\text{cut}, \text{min}}^2$ introduced after Eq. (11). The results of **TOY-TAG** not being reliable to high accuracy for small values of mass drop does not have such dramatic consequences since the typical values used for this tagger in studies involving jet substructure are above 0.6 [3].

The quality of the description of S/B by **TOY-TAG** is slightly worse and not so generic. It is different for different taggers and it depends on the values of the parameters. In particular, for taggers independent of the mass and transverse momentum of the jet, Eqs. (13)-(18), the agreement between **TOY-TAG** and tagging in MC is remarkable when the unclustering is performed with the k_t -algorithm, and remains within 20% with respect to true C/A tagging, provided that no extreme values of the tagging parameters are used (for instance, for $J_{p_T, \text{cut}} > 0.03$, the reliability of the interactive tagger tool is deficient). On the other hand, the agreement between **TOY-TAG** and true tagging on MC deteriorates for taggers which depend on mass and p_T of the jet. As shown before, for the y_{cut} tagger, the description by the **TOY-TAG** remains within $\sim 30\text{-}40\%$ for moderate values of the tagger and a similar statement can be applied to mass drop. The user should be aware of such limitations (at high and low values of the parameters) at all times.

The real jet substructure is obviously more complex than what can be inferred from the relevant splitting. We would like to emphasize that our objective was not to construct a tool which would replace dedicated jet substructure analysis but rather to deliver a simple program which is able to provide some insight into what happens when a particular tagger is applied to an ensemble of signal or background events. At the same time, as discussed in this section, it is capable of providing semi-quantitative (and often even fairly accurate) results for S/B and S/\sqrt{B} . Dedicated analysis cannot be replaced if one wants to properly optimize the taggers but they often resemble black boxes and a lot of information about how the taggers act on a particular event set is inaccessible. This information can be obtained with our **TOY-TAG**, which in other words means that the tool that we provide is complementary to the above mentioned dedicated substructure analyses.

4 Studying taggers with **TOY-TAG**

The results presented in this section are extracted from the interactive tagger tool **TOY-TAG** introduced and validated in the previous section. We use **TOY-TAG** to illustrate and discuss features of the taggers. All results shown in this section were obtained with the $p_{T, \text{min}} = 400 \text{ GeV}$ cut on jets, although similar conclusions are valid for higher values of $p_{T, \text{min}}$.

Fig. 4 shows the (z, Δ) histograms for the relevant splitting of the signal and background jets obtained with the selection criteria from section 2.1⁶. It illustrates the main difference in the substructure between the Z-jets and the QCD jets. For the case of hadronically decaying Z, most of the events gather near $z \sim \frac{1}{2}$ whereas the QCD events are concentrated close to $z \sim 0$ and $z \sim 1$. This is the difference that essentially all taggers try to exploit in order to keep the most of the signal events and reject the most of the background events. Another difference between the signal and the background events is that the latter are much more abundant which can be seen by comparing the color scale in the histograms in Fig. 4.

Since the majority of the background events concentrates at small momentum fraction and large angles, those taggers which are able to reject that region of the (z, Δ) plane will be preferred. Also, signal events are mostly symmetric, hence removing the mentioned portion of the plane will not decrease the signal too much. In the region of more symmetric z , the background events have smaller values of Δ than the signal events. We note in particular that some of the background events have very small Δ which, based on Eq. (7), could naively suggest that the corresponding jet mass is below the cut used in the selection. We checked that those jets are massive enough to pass the selection because their subjets have finite masses which should not be neglected. In other

⁶In particular the U-type shape of the histogram results from the window cut on the mass of the jet.

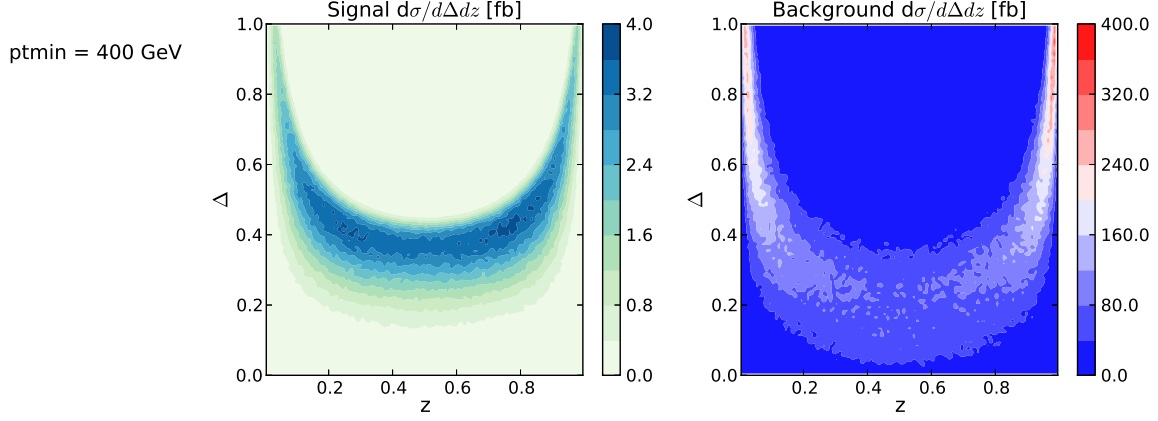


Figure 4: Histograms of (z, Δ) of the relevant splitting for signal and background events with the criteria from sec. 2.1. The fat jet is found with the k_t algorithm with $R=1$.

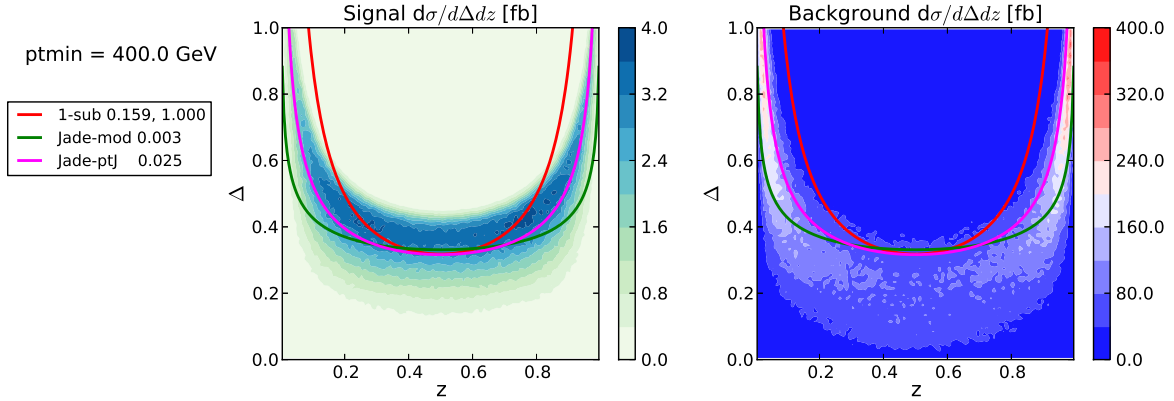


Figure 5: Comparison of taggers independent (within our approximations) of p_{TJ} and m_J . The fat jet is found with the k_t algorithm with $R=1$. In the case of 1-subjecttiness the angular weighting exponent was set to $\beta = 1$.

words, the massless subjet formula (7) is too crude an approximation for the background jets and one obtains much more realistic results with jet mass computed from Eq. (10). This is precisely what we use, for those taggers which depend explicitly on m_J , in our implementations in **TOY-TAG**, as discussed in section 2.4 and at the beginning of section 3. Putting the above things together, we can conclude that those taggers for which the functional form of $\Delta(z)$ present a sharp slope at low z and $1 - z$, and a rather flat behavior in the intermediate region, will provide best cleaning of the signal.

4.1 The taggers: differences and similarities

Fig. 5 illustrates the first group of taggers, namely those which do not depend on the jet mass and jet transverse momentum. These are: 1-subjecttiness, Jade distance normalized to p_{TJ} and the modified Jade distance. We remind the reader that for each curve, all events above it, that is those having larger Δ for a given z , are kept by the tagger and all events below are rejected. This is true for all the taggers discussed in this paper except for pruning as will be explained later. As can be seen from Eqs. (13), (14) and (15), the main difference in the definition of those taggers is in the power of Δ . Fig. 5 is an example showing what happens if we decide that we want to keep the same level of symmetric events with $z \sim \frac{1}{2}$ with each of these three taggers. We see that is such a case the events with low z or $1 - z$ are the most effectively removed the lower the Δ power in the tagger definition. That is why 1-subjecttiness leaves almost no background events whereas modified Jade accepts most of them. As we see in Fig. 5, the situation is more complex

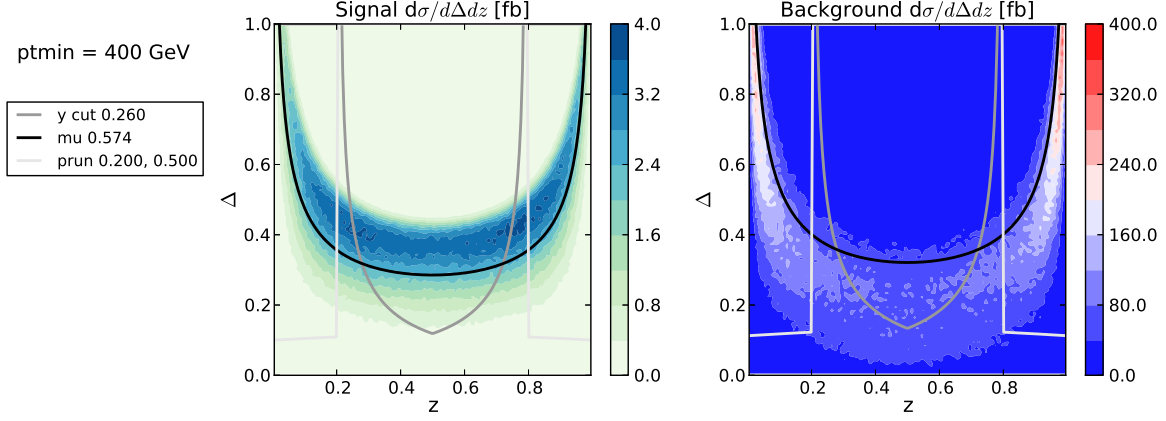


Figure 6: Comparison of three distinctly different taggers: mass drop, asymmetry cut and pruning. The fat jet is found with the k_t algorithm with $R=1$.

however since 1-subjettiness tends to remove also a significant part of the signal events that we would like to keep, so it may turn out that it is more preferable to use Jade-pTj which, due to its shape accepts much of the signal events. This dilemma can be solved by computing the ratios of signal/background and signal/ $\sqrt{\text{background}}$ which we shall do in the following subsection.

Fig. 6 shows three distinctly different taggers: mass drop, asymmetry cut and pruning. Each of them is taken at an example value of the parameter(s) for illustration. All events above the curve, for mass and ycut, and below the pruning curve are accepted. We see that the mass drop follows closely the shape of the color maps but in such a way that most of the signal events are above the curve and most of the background events below. On the contrary, the asymmetry cut and the pruning have very different shapes than the histograms. These taggers are focused on removing the low z and low $1-z$ events and this is the main feature that they have in common. We see from Fig. 6 that they could even mimic one another in certain subregions of the parameter space. The main difference between pruning and asymmetry cut, as illustrated in the figure, is that the latter also removes part of the background events which are symmetric in z . This feature comes from the fact that, as already mention in sec. 2.4, the asymmetry cut tagger, even in its simplified version from Eq. (12), entangles Δ and z whereas pruning cuts on each of them separately. It is interesting to note that the mass drop tagger and the asymmetry tagger or pruning are complementary and one should expect to improve performance by combining them as it was indeed done in a number of analyses [3, 18].

4.2 Purity, significance and combinations of taggers

One of the useful features of TOY-TAG is that it can compute the purity of the signal, S/B , and the significance, S/\sqrt{B} , for the simulated events and the modelled taggers. This allows one to get a first estimate of the performance of the taggers as a function of their parameters and, most importantly, to study potential gains to be had by combining different taggers.

In Fig. 5 we had three different taggers with the parameters chosen such that they accept similar number of events near $z \sim \frac{1}{2}$. The corresponding purity and significance values ($S/B, S/\sqrt{B}$) are: (0.091, 0.71) for 1-subjettiness, (0.057, 0.82) for Jade-pTj and (0.03, 0.65) for modified Jade. As expected from the figure, we see that the modified Jade performs the worst simply because it accepts too many background events with low z or low $1-z$. On the contrary “1-sub” and “Jade-pTj” reject most of those events which results in much better performance in terms of S/B and S/\sqrt{B} . It is also interesting to note that even though 1-subjettiness rejects more of the signal events near $z \sim \frac{1}{2}$ compare to the “Jade-pTj” it still does better than the latter due to the fact that it also removes more of the background events.

TOY-TAG allows for a scan over the full range of the tagger parameter, which makes it easy to study S/B vs. S/\sqrt{B} relation. Some examples of such plots are shown in Fig. 7. Even though these results should be regarded as semi-quantitative, they provide useful information about the expected trends as well as first estimates which can help identifying potentially interesting ranges

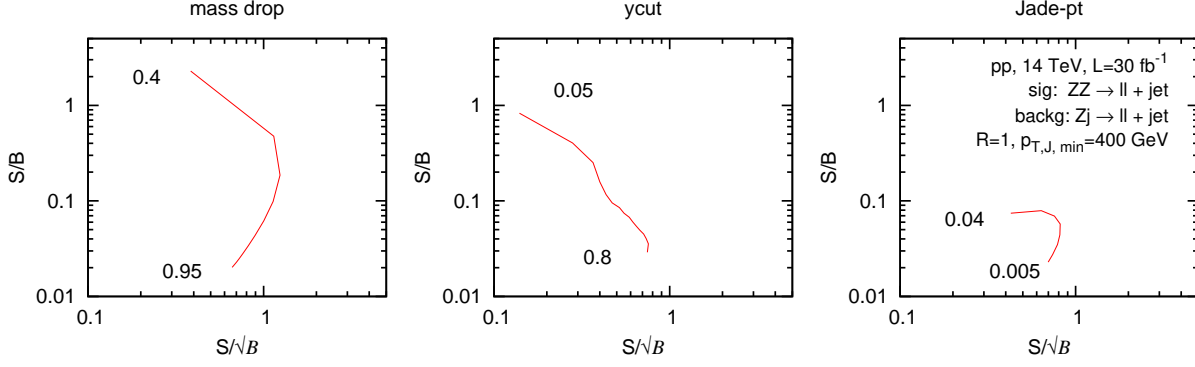


Figure 7: S/B vs. S/\sqrt{B} for different taggers applied to jets with $p_T > 400\text{GeV}$. The numbers in the plots correspond to the values of tagger parameter at the extremes of each curve.

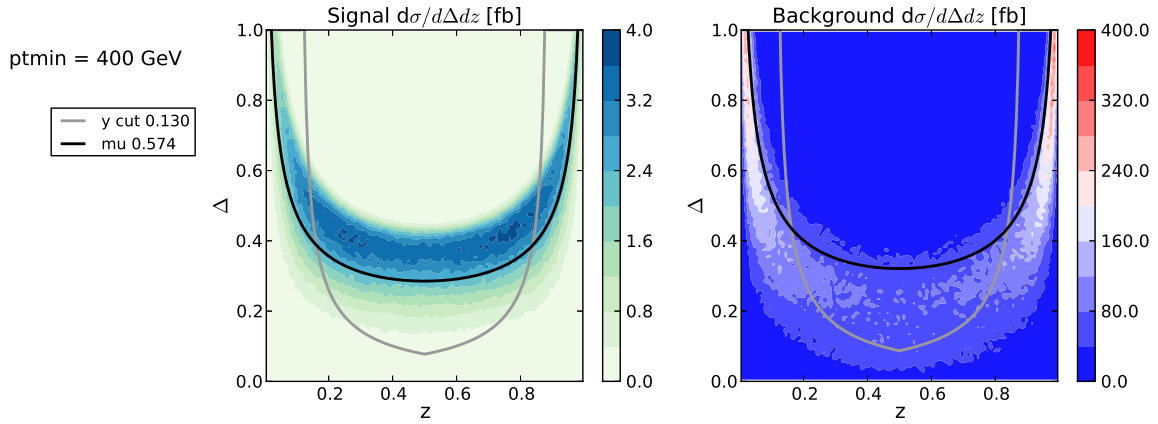


Figure 8: Combination of mass drop and asymmetry cut. The fat jet is found with the k_t algorithm with $R=1$.

of tagger parameter.

Another interesting question that can be studied with **TOY-TAG** is what happens to purity and significance when two taggers are combined. An illustration is given in Fig. 8 for the mass drop and asymmetry cut. It is clear from that figure that the asymmetry cut alone does very well for the events with low z and $1-z$ by rejecting a lot of background in that region. However, y_{cut} alone, still keeps many relatively symmetric background events with low Δ . Those events could be rejected by imposing higher values of the y_{cut} parameter but that would lead to a drastic drop of the signal events as well. However, if the mass drop is added on the top of the asymmetry tagger, most of these low Δ background events are rejected while most of the corresponding signal events in that region are kept. That allows one to improve the performance. In terms of the $(S/B, S/\sqrt{B})$ pair we have $(0.039, 0.75)$ for y_{cut} alone, $(0.073, 1.1)$, for mass drop alone and $(0.11, 1.1)$ for the combination. Hence, we see that by combining the two tagger we were able to improve the purity of our signal while keeping the same significance.

5 Summary

The difference between substructure of boosted jets coming from decays of heavy objects and that of the QCD jets is widely used as a powerful tool to discriminate between signal and background in searches for heavy objects. The real substructure of jets is complex and full algorithmic implementations of taggers often turn them into a black box, seriously limiting the chance of understanding of what actually happens to the ensemble of the signal and background events. This is inevitable if one aims at optimizing an analysis for the highest performance. However, it is also interesting to try to obtain some insight into what happens when a particular tagger or a group of taggers is

applied.

In this paper, we explicitly studied how jet substructure taggers act on a set of signal and background events. We considered $ZZ \rightarrow l^+l^- + \text{jet}$ as signal and $Z + \text{jet} \rightarrow l^+l^- + \text{jet}$ as background. In order to be able to compare all the taggers within a single framework we studied only how they act on the most relevant splitting in a jet, that is the one which is responsible for most of the jet mass. We have checked that this approximation grasps the most important features and it allows for a semi-quantitative analysis.

We developed an interactive tool, **TOY-TAG**, that allows one to apply approximate versions of the different taggers, or their combinations, to the signal and background files and to study what happens when the tagger parameters are varied. It also provides estimates for the ratios of signal/background and signal/ $\sqrt{\text{background}}$. For some taggers, we introduced extra modeling, which involved mass of the heavier subjet, and which allowed us to reproduce important features of the exact versions of the taggers. We view **TOY-TAG** as being complementary to dedicated substructure analyses as it can provide some guidance and understating of the way a particular tagger acts on an set of signal and background events.

We used our tool to discuss main differences between taggers. We illustrated how various definitions of taggers translate into the regions of (z, Δ) of the relevant splitting that are accepted or rejected. We identified the areas where different taggers overlap. On the other side, we emphasized which distinct differences between the taggers lead to an improvement of performance when several taggers are combined.

We believe that **TOY-TAG**, in its current form, can serve many more analyses. We also plan to extend it such that it is able to handle broader class of input signal and background files as well as to apply any tagger defined as a function $\Delta(z)$. The **TOY-TAG** tool is available from the website <http://www.ipp.dur.ac.uk/~sapeta/toytag>.

Acknowledgements

We are grateful to G. Soyez for useful discussions throughout the development of this work. We thank M. Cacciari and G. Salam for their valuable comments on the manuscript and the **TOY-TAG** tool. We thank J. Thaler for pointing out the generalized formulation of N-subjettiness. The work of PQA is supported by the French ANR under contract ANR-09-BLAN-0060.

References

- [1] J. M. Butterworth, B. E. Cox, and Jeffrey R. Forshaw. *WW* scattering at the CERN LHC. *Phys. Rev.*, D65:096014, 2002.
- [2] Michael H. Seymour. Searches for new particles using cone and cluster jet algorithms: A Comparative study. *Z.Phys.*, C62:127–138, 1994.
- [3] Jonathan M. Butterworth, Adam R. Davison, Mathieu Rubin, and Gavin P. Salam. Jet substructure as a new Higgs search channel at the LHC. *Phys.Rev.Lett.*, 100:242001, 2008.
- [4] Tilman Plehn, Gavin P. Salam, and Michael Spannowsky. Fat Jets for a Light Higgs. *Phys.Rev.Lett.*, 104:111801, 2010.
- [5] Graham D. Kribs, Adam Martin, Tuhin S. Roy, and Michael Spannowsky. Discovering Higgs Bosons of the MSSM using Jet Substructure. *Phys.Rev.*, D82:095012, 2010.
- [6] Jason Gallicchio, John Huth, Michael Kagan, Matthew D. Schwartz, Kevin Black, et al. Multivariate discrimination and the Higgs + W/Z search. *JHEP*, 1104:069, 2011.
- [7] Davison E. Soper and Michael Spannowsky. Combining subjet algorithms to enhance ZH detection at the LHC. *JHEP*, 1008:029, 2010.
- [8] Peter Richardson and David Winn. Investigation of Monte Carlo Uncertainties on Higgs Boson searches using Jet Substructure. *Eur.Phys.J.*, C72:2178, 2012.
- [9] David E. Kaplan, Keith Rehermann, Matthew D. Schwartz, and Brock Tweedie. Top Tagging: A Method for Identifying Boosted Hadronically Decaying Top Quarks. *Phys.Rev.Lett.*, 101:142001, 2008.
- [10] Stephen D. Ellis, Christopher K. Vermilion, and Jonathan R. Walsh. Techniques for improved heavy particle searches with jet substructure. *Phys.Rev.*, D80:051501, 2009.

- [11] Stephen D. Ellis, Christopher K. Vermilion, and Jonathan R. Walsh. Recombination Algorithms and Jet Substructure: Pruning as a Tool for Heavy Particle Searches. *Phys.Rev.*, D81:094023, 2010.
- [12] Tilman Plehn and Michael Spannowsky. Top Tagging. *J.Phys.*, G39:083001, 2012.
- [13] David Krohn, Jesse Thaler, and Lian-Tao Wang. Jet Trimming. *JHEP*, 02:084, 2010.
- [14] A. Altheimer, S. Arora, L. Asquith, G. Brooijmans, J. Butterworth, et al. Jet Substructure at the Tevatron and LHC: New results, new tools, new benchmarks. *J.Phys.*, G39:063001, 2012.
- [15] D0 Collaboration. Victor Mukhamedovich Abazov et al. Measurement of color flow in $t\bar{t}$ events from $p\bar{p}$ collisions at $\sqrt{s} = 1.96$ TeV. *Phys.Rev.*, D83:092002, 2011.
- [16] Serguei Chatrchyan et al. Studies of jet mass in dijet and $W/Z + \text{jet}$ events. *JHEP*, 1305:090, 2013.
- [17] Georges Aad et al. Jet mass and substructure of inclusive jets in $\sqrt{s} = 7$ TeV pp collisions with the ATLAS experiment. *JHEP*, 1205:128, 2012.
- [18] Yanou Cui, Zhenyu Han, and Matthew D. Schwartz. W-jet Tagging: Optimizing the Identification of Boosted Hadronically-Decaying W Bosons. *Phys.Rev.*, D83:074023, 2011.
- [19] Torbjorn Sjostrand, Stephen Mrenna, and Peter Z. Skands. PYTHIA 6.4 Physics and Manual. *JHEP*, 0605:026, 2006.
- [20] S. Catani, Yuri L. Dokshitzer, M.H. Seymour, and B.R. Webber. Longitudinally invariant K_t clustering algorithms for hadron hadron collisions. *Nucl.Phys.*, B406:187–224, 1993.
- [21] Yuri L. Dokshitzer, G.D. Leder, S. Moretti, and B.R. Webber. Better jet clustering algorithms. *JHEP*, 9708:001, 1997.
- [22] M. Wobisch and T. Wengler. Hadronization corrections to jet cross-sections in deep inelastic scattering. hep-ph/9907280, 1998.
- [23] Matteo Cacciari and Gavin P. Salam. Dispelling the N^3 myth for the k_t jet-finder. *Phys.Lett.*, B641:57–61, 2006.
- [24] Matteo Cacciari, Gavin P. Salam, and Gregory Soyez. FastJet user manual. *Eur.Phys.J.*, C72:1896, 2012.
- [25] Matteo Cacciari, Gavin P. Salam, and Gregory Soyez. <http://www.fastjet.fr>.
- [26] J.M. Butterworth, John R. Ellis, and A.R. Raklev. Reconstructing sparticle mass spectra using hadronic decays. *JHEP*, 0705:033, 2007.
- [27] Jonathan M. Butterworth, John R. Ellis, Are R. Raklev, and Gavin P. Salam. Discovering baryon-number violating neutralino decays at the LHC. *Phys.Rev.Lett.*, 103:241803, 2009.
- [28] Jesse Thaler and Ken Van Tilburg. Identifying Boosted Objects with N-subjettiness. *JHEP*, 1103:015, 2011.
- [29] Iain W. Stewart, Frank J. Tackmann, and Wouter J. Waalewijn. N-Jettiness: An Inclusive Event Shape to Veto Jets. *Phys.Rev.Lett.*, 105:092002, 2010.
- [30] Jesse Thaler and Ken Van Tilburg. Maximizing Boosted Top Identification by Minimizing N-subjettiness. *JHEP*, 1202:093, 2012.